NANO LETTERS
Cite This: Nano Lett. XXXX, XXX, XXX−XXX
Letter
pubs.acs.org/NanoLett

Dronpa: A Light-Switchable Fluorescent Protein for Opto-Biomechanics

Res Jöhr,* Magnus S. Bauer, Leonard C. Schendel, Carleen Kluger, and Hermann E. Gaub*

Lehrstuhl für Angewandte Physik and Center for Nanoscience, Ludwig-Maximilians-Universität, Munich 80799, Germany

Supporting Information

ABSTRACT: Since the development of the green fluorescent protein, fluorescent proteins (FP) are indispensable tools in molecular biology. Some FPs change their structure under illumination, which affects their interaction with other biomolecules or proteins. In particular, FPs that are able to form switchable dimers became an important tool in the field of optogenetics. They are widely used for the investigation of signaling pathways, the control of surface recruitment, as well as enzyme and gene regulation. However, optogenetics did not yet develop tools for the investigation of biomechanical processes. This could be leveraged if one could find a light-switchable FP dimer that is able to withstand sufficiently high forces. In this work, we measure the rupture force of the switchable interface in pdDronpa1.2 dimers using atomic force microscopy-based single molecule force spectroscopy. The most probable dimer rupture force amounts to around 80 pN at a pulling speed of 1600 nm/s. After switching of the dimer using illumination at 488 nm, there are hardly any measurable interface interactions, which indicates the successful dissociation of the dimers. Hence this Dronpa dimer could expand the current toolbox in optogenetics with new opto-biomechanical applications like the control of tension in adhesion processes.

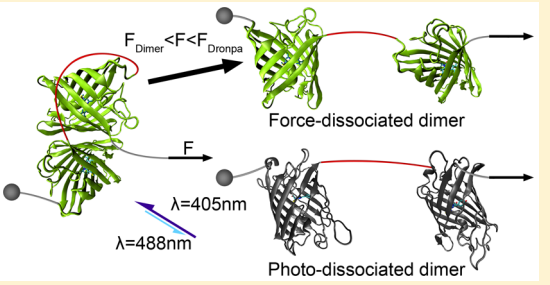

KEYWORDS: *Optogenetics, biomechanics, Dronpa, single molecule force spectroscopy, atomic force microscopy*

Light-switchable fluorescent proteins (ls-FP) like the green fluorescent protein (GFP) have become an essential tool in biology for imaging and tracking of processes inside cells.[1−5] Beyond that, optogenetic methods employ them to even dynamically control such processes.[6−8] These tools exploit the fact that ls-FPs change their structure upon irradiation with light of a suitable wavelength. Since the protein function is directly encoded in its structure, this alters the way the FP interacts with its environment. For example, light alters the affinity of light-inducible dimerizers to the corresponding ligand. Hence, the association of these dimers can be directly controlled using light pulses.[9−12] This has been utilized for subcellular localization of proteins[13−15] as well as gene and enzyme regulation.[6,16,17] In the broader context, optogenetic tools have been employed for achieving synaptic control and to study signaling network dynamics.[8]

This list of potential applications, however, does not include methods for biomechnical investigations. It is known that many processes in cells are controlled by forces.[18,19] Cells continuously sense their environment using mechanosensors in the cell membrane, i.e., the focal adhesions. From there, the signals are transduced and affect the organization of the cytoskeleton and with it the cell shape or cell migration and also more complex processes like cell division and differentiation.[20−27] So far, such processes could be potentially investigated using static FP force sensors that lose their fluorescence when unfolded[28−30] or FRET based tension sensors. However, this does not allow for dynamic control or triggering of force-induced reactions, e.g., by revealing a cryptic binding site.[31] This lack of mechanobiology applications in the optogenetics toolbox could be diminished if robust ls-FPs with a sufficiently high interface rupture force could be found or designed.

In this work, we investigate the ls-FP Dronpa, which is known from optogenetics.[17,32,33] It is derived from a tetrameric FP found in Pectiniidae corals and has a characteristic β-barrel structure similar to GFP.[34] It has a remarkable photostability and was shown to be switchable more than 50 times between its dark and bright fluorescent state.[35] The binding interfaces were further modified to yield a dimeric Dronpa variant.[17] This variant has successfully been used to control the accessibility of the active site of kinases and thus their activity as well as for gene regulation.[32,33] Here we investigate the interface interaction in the pdDronpa1.2 dimer[32] (see Figure 1a), by using atomic force microscopy (AFM)-based single molecule force spectroscopy (SMFS). The results reveal a most probable interface rupture force of 80 pN in the bright state that is no longer detectable when switched to the dark state. Hence the dimer association can be controlled by light as well as by force. This opens the way for possible applications of this system in biomechanics studies.

Received: February 13, 2019
Revised: March 25, 2019
Published: March 26, 2019

DOI: 10.1021/acs.nanolett.9b00639
Nano Lett. XXXX, XXX, XXX−XXX

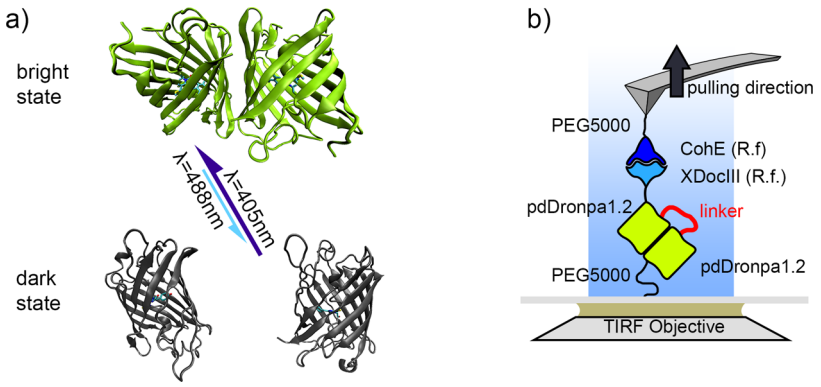

Figure 1. (a) Crystal structure of the fluorescent and dark state of Dronpa (PDB: 6D39 (bright) and 2POX (dark)). The bright state can be switched to the dark one by intense irradiation with blue light (λ = 488 nm). The backswitching is triggered by dim light at 405 nm. (b) Scheme of the experimental setup used for AFM-based SMFS.

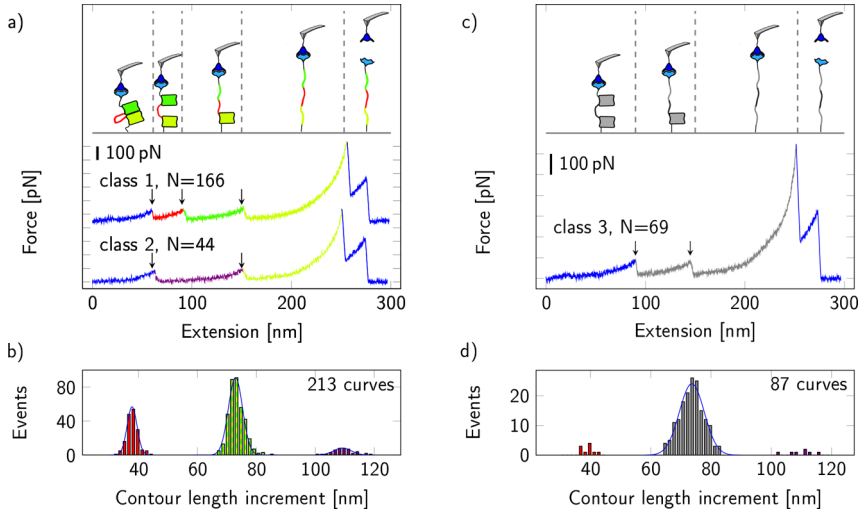

Figure 2. Exemplary force extension curves and contour length histograms with Gaussian fits from SMFS of the pdDronpa1.2 dimer. Unfolding events that are specific for the Dronpa dimer are indicated with arrows. Blue parts are from the PEG stretching as well as the specific XDocIII/CohE rupture. (a and b) Results of pdDronpa1.2 dimers prepared in the bright state. The red part represents the interface rupture, and the green parts represent the pdDronpa1.2 unfolding. Dronpa domains were colored slightly differently to enhance the readability of the scheme. Violet indicates the events with a supposed simultaneous rupture of the interface and unfolding of one Dronpa subunit. (c and d) Results of pdDronpa1.2 dimers prepared in the dark, nonbinding state. The fit parameters are available in the Supporting Information.

Results and Discussion. In order to characterize individual pdDronpa1.2 homodimers by SMFS, we designed a protein construct, where we linked two Dronpa domains with a flexible linker.[36] The dimer was further fused to a pulling handle, a strategy that has already been successfully applied to probe the unfolding of individual proteins.[37,38] The linker was made out of 73 amino acids, which corresponds to a contour length increment of ca. 28 nm. This increment can be easily detected in SMFS and thus facilitates the direct and simultaneous identification of the interface rupture event and the unfolding of the individual Dronpa domains in a single experiment. Figure 1b shows the complete scheme of the SMFS measurement. The protein construct is clamped between the AFM cantilever and the sample surface and then pulled apart.[38,39] The specificity of the measurement is granted by using the XDocIII/CohE cohesin dockerin receptor ligand pair from *R. flavefaciens* as a protein handle.[40] Both proteins, the Dronpa dimer and the CohE, were covalently attached to the cantilever and the sample, respectively, using polyethylene glycol (PEG) spacers with a molecular weight of 5000 Da. Switching of the Dronpa dimer was achieved via total internal reflection (TIR) illumination from below the sample slide. Initially the sample was illuminated with 405 nm light for a short instance (5 s) to prepare the proteins in the bright state that allows for intramolecular domain association. In the second part of the experiment, the sample was intermittently illuminated with 488 nm light in order to switch the domains to their dark state and to trigger dissociation of the Dronpa domains.

The force extension curves from the SMFS measurement were filtered using the specific XDocIII/CohE fingerprint interaction. A total of 213 specific curves was obtained for the domains that were prepared in the bright state (i.e., after 405 nm illumination). They could be classified into two main classes. Examples of the force extension curves are shown in Figure 2a. Besides the characteristic peak from the XDocIII/CohE rupture, the first class contains 166 curves that show three characteristic peaks (indicated with arrows in Figure 2a). Remarkably, these rupture events had similar unfolding forces of around 80 pN. The second class contained 44 curves and revealed only two peaks with similar unfolding forces. The measurement of the dark state dimers yielded 87

DOI: 10.1021/acs.nanolett.9b00639
Nano Lett. XXXX, XXX, XXX−XXX

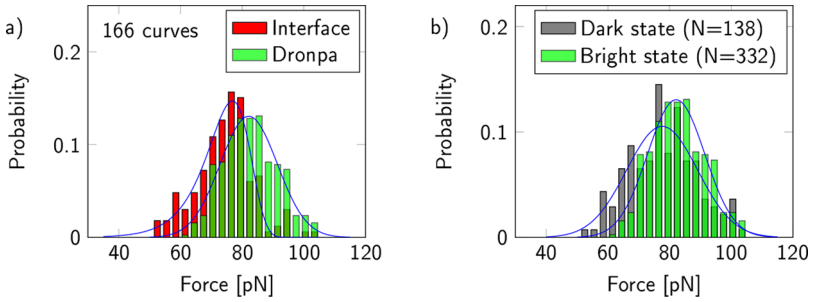

Figure 3. Normalized rupture force histograms from SMFS. The distribution of the interface rupture was fitted using the Bell−Evans model. The histograms of the Dronpa unfolding were fitted with normal distributions. (a) Distributions for the Dronpa in the bright state and for the interface. (b) Comparison of histograms for Dronpa after illumination with 405 nm (bright state) and 488 nm (dark state). The dark state histogram was composed of curves without an interface rupture event. It presumably contains a contribution from dissociated Dronpa domains in the bright state. The fit parameters are given in the Supporting Information.

specific curves (Figure 2c,d). Most of the (N = 69) curves belong to a single class with two Dronpa related peaks.

The contour length increments l_c of the force peaks were calculated from fits based on the worm-like chain model with a fixed persistence length of 0.4 nm. The results for the bright state experiment are displayed in the histogram in Figure 2b. They reveal peaks at 37.8, 72.9, and 109.2 nm. The peak at 73 nm is found in all curve classes. If we consider the l_c of a single amino acid to be around 0.35−0.38 nm[41] and take into account that Dronpa has about 210 structured amino acids with an end-to-end distance of 2.5 nm, it follows that the expected l_c for Dronpa unfolding is in the range from 71 to 77 nm. This is in good agreement with our experimental value. Therefore, we attribute this force peak to the unfolding of the Dronpa domains. The remaining peaks at 37.8 and 109.2 nm in Figure 2b can be explained with the rupture of the interface. The peak at 37.8 nm is solely attributed to the linker that connects the two Dronpa domains. Hereby we note that the measured contour length increment of the linker is indeed longer than the expected 28 nm calculated from the primary structure. However, this conclusion is justified because we have to include the unstructured amino acids from the two Dronpa domains that were excluded from the previous calculation of the Dronpa contour length. The contour length increment of 109.2 nm can, however, not be explained by a single domain unfolding event. Since its length corresponds to the sum of one Dronpa unfolding and the dimer interface, we suggest that this unfolding event is linked to the rupture of the dimer and simultaneous unfolding of one of the Dronpa domains. This is further corroborated by the fact that the unfolding of the single Dronpa was always observed after the event with l_c = 109.2 nm (see Figure 2a). As we will show later, it is likely that the Dronpa domain unfolds first and consequently induces the rupture of the interface.

In contrast, Figure 2c shows that curves with force peaks associated with the interface, i.e., contour length increments of 37.8 and 109.2 nm, were significantly reduced after illumination at 488 nm (see Figure 2d). Analysis of the force extension curves reveals that 80% of the curves (69 out of 87 curves) show only the characteristic signature of the unfolding of two Dronpa domains but no interface rupture (see Figure 2c). The remaining 18 curves showed characteristic force distance traces similar to the ones of the associated dimers shown in Figure 2a. This indicates that the dimer is either in an associated or dissociated state. Potential intermediate states with a lower rupture force, for example, in mixed dimers, where one of the domains is in the bright and the other in the dark state, could not be detected. If they exist, they are expected to be relatively weak. Hence we suggest that the dimer behaves as an effective two-state system, where the interface rupture can only be observed using AFM if both Dronpa domains are in the bright state and associated. This behavior would be favorable for potential applications. It facilitates the dissociation under blue light and would compensate for the low quantum efficiency for the switching from the bright to the dark state (QE_{bd} = 0.00032), which is much lower than vice versa (QE_{db} = 0.37).[34,42] We note that the observed two-state behavior might be an oversimplification of the actual processes. For example, we have no data on the fluorescence during individual pulling experiments and thus cannot exclude that the Dronpa domains lose their fluorescence during the interface rupture. However, since the determined l_c is in good agreement with the expected tertiary structure of the bright state, we assume that the domains remain functional.

In order to understand the mechanics of the dimer rupture, i.e., the proposed simultaneous rupture of the interface and the unfolding of the Dronpa domain, we analyzed the corresponding rupture force distributions (Figure 3a). The distribution of the interface was fitted using the Bell−Evans model.[43,44] The most probable rupture force for the selected pulling speed of 1600 nm/s was 76.9 ± 1.1 pN, which is comparable to photochemical single molecule switches.[45−47] The histogram of the Dronpa unfolding was fitted using a normal distribution with a most probable rupture force of 82.1 ± 1.1 pN. Hence, the individual Dronpa domain is only slightly more stable than the interface. Its unfolding force is comparable to other fluorescent proteins with a β-barrel structure.[28,48] Because of the overlap of the two force distributions, it follows that unfolding of a Dronpa domain might occur before the rupture of the interface as was also suggested from the experiments.

Comparing the rupture force probability distributions of the dark and bright states shown in Figure 3b, one observes that they are slightly shifted with respect to each other. The dark state distribution has a maximum at 77.6 ± 2.5 pN and a standard deviation of σ = 10.3 pN. It is thus weaker and has a broader distribution compared to the bright state with 82.1 ± 1.1 pN and σ = 9.3 pN. The lower unfolding force is in agreement with research from Mizuno et al. where they found that illumination of Dronpa with blue light causes flexibility of the seventh β-strand inside the β-barrel structure, thus probably weakening the protein fold (see Figure 1a).[49] This effect might facilitate the dissociation of the dimer if it is

DOI: 10.1021/acs.nanolett.9b00639
Nano Lett. XXXX, XXX, XXX−XXX

switched to the dark state. The fact that there is a difference between the two distributions is further evidence that the fluorescent Dronpa domains remain in their bright state during interface rupture.

In summary, we investigated light-switchable pdDronpa1.2-linker-pdDronpa1.2 protein constructs using AFM-based SMFS. At a retraction speed of 1600 nm/s, we found that the interface is able to withstand a force of around 80 pN. This is a relatively high stability, considering that the dimer is supposed to be stabilized by hydrophobic interactions.[17] It is notable that most Dronpa domains keep their fold during interface rupture. Comparing to studies of other β-barrel FPs, this suggests that Dronpa dimers are likely to remain functional and associated under the tensile stress that is prevalent under physiological conditions.[28,50] Further, the dimer could be dissociated under illumination with 488 nm light. The interface interaction was hardly observed in this case anymore. Taking into account the loading rate dependence of the interface strength, we expect a rupture force in the range 20−30 pN under physiological conditions.[51] This rupture force of the Dronpa dimer lies above the range of forces that are typically observed in mechanotransduction and signaling[31,52−54] but is significantly weaker than the forces found during bacterial adhesion, which can amount to several hundred pNs.[40,55,56] We thus believe that our results have strong implications for applications in the study of mechanotransduction and signaling. Dronpa is sufficiently strong to be used for manipulation of the conformation of focal adhesion proteins without the interface being pulled open. One potential application to achieve this would be the incorporation of Dronpa dimers into stretchable proteins such as talin that have cryptic binding sites, which are only accessible under tension.[31] Exchange of such cryptic domains with Dronpa dimers that hold the cryptic domain in the linker region would protect this binding site from tension forces so that reactions triggered by binding to this site become controllable by light. Our study further shows a new way to combine force application and light-induced conformational switching in AFM-SMFS as a tool by itself. This opens up the road for experiments, which employ dynamic force probes with properties that can be switched during the experiment.

Experimental Section. The experimental procedures for this study were adapted from previously published protocols.[38,39,57,58] Detailed information is given in the Supporting Information.

Protein Synthesis. The pdDronpa1.2-linker-pdDronpa1.2 constructs with the N-terminal ybbR-hexahistidine tag and C-terminal XDocIII domain from *R. flavefaciens* were assembled and subcloned into peT28a plasmids via Gibson assembly. The protein was expressed in *E. coli* NiCo21(DE3) cells using an autoinduction medium and then harvested and purified employing a standard protocol including Ni-NTA affinity chromatography.

Sample Preparation. Cover glasses were cleaned and silanized using (3-aminopropyl)-dimethyl-ethoxysilane. The amine functionalized surface was subsequently conjugated with NHS-PEG-maleimide spacers. The maleimide was reacted with Coenzyme A in order to allow Sfp phosphopantetheinyl transferase-mediated coupling to the ybbR tag of the Dronpa construct.

SMFS Measurement. Single molecule force spectroscopy was performed on a home-built TIRF-AFM.[59] TIR illumination was used for switching of the Dronpa domains, which restricted the excitation to a volume within 100 nm above the sample surface. A glucose oxidase-based oxygen scavenging system (25 U/mL glucoseoxidase, 1700 U/mL catalase, and 0.6% w/v glucose) was used in order to prevent bleaching of the Dronpa domains.

Data Analysis. Force extension curves were processed and filtered in a semiautomated way.[39] Drift compensation and peak identification was done for all curves with a tip sample interaction. The contour length increments of individual unfolding events were determined with the WLC model using a persistence length of 0.4 nm.[60] Specific curves were identified by selecting the ones that showed the characteristic rupture signature between the XDocIII handle and the CohE pulling domain[40] as well as the pdDronpa1.2 specific peak.

■ ASSOCIATED CONTENT

Supporting Information

The Supporting Information is available free of charge on the ACS Publications website at DOI: 10.1021/acs.nanolett.9b00639.

Fit parameters for the contour length distributions and the rupture force histograms, materials and methods used for recombinant protein synthesis, sample preparation, and single molecule force spectroscopy measurements (PDF)

■ AUTHOR INFORMATION

Corresponding Authors

*E-mail: res.joehr@lmu.de.
*E-mail: gaub@lmu.de.

ORCID

Res Jöhr: 0000-0002-6204-5410
Leonard C. Schendel: 0000-0002-1986-2693
Hermann E. Gaub: 0000-0002-4220-6088

Notes

The authors declare no competing financial interest.

■ ACKNOWLEDGMENTS

The authors thank T. Nicolaus for laboratory support, L.F. Milles for providing the linker sequence of the Dronpa dimers, and E. Durner and W. Ott for preparing the CohE protein constructs used for specific protein pulling during AFM-based SMFS experiments. We acknowledge funding from the German Research Foundation within the framework of the SFB1032.

■ REFERENCES

(1) Tsien, R. Y. The green fluorescent protein. *Annu. Rev. Biochem.* **1998**, *67*, 509−544.
(2) Nienhaus, K.; Ulrich Nienhaus, G. Fluorescent proteins for live-cell imaging with super-resolution. *Chem. Soc. Rev.* **2014**, *43*, 1088−1106.
(3) Chang, H.; Zhang, M.; Ji, W.; Chen, J.; Zhang, Y.; Liu, B.; Lu, J.; Zhang, J.; Xu, P.; Xu, T. A unique series of reversibly switchable fluorescent proteins with beneficial properties for various applications. *Proc. Natl. Acad. Sci. U. S. A.* **2012**, *109*, 4455−4460.
(4) Moeyaert, B.; Nguyen Bich, N.; De Zitter, E.; Rocha, S.; Clays, K.; Mizuno, H.; van Meervelt, L.; Hofkens, J.; Dedecker, P. Green-to-Red Photoconvertible Dronpa Mutant for Multimodal Super-resolution Fluorescence Microscopy. *ACS Nano* **2014**, *8*, 1664−1673.
(5) Zhou, X. X.; Lin, M. Z. Photoswitchable fluorescent proteins: ten years of colorful chemistry and exciting applications. *Curr. Opin. Chem. Biol.* **2013**, *17*, 682−690.

DOI: 10.1021/acs.nanolett.9b00639
Nano Lett. XXXX, XXX, XXX−XXX

(6) Zhang, K.; Cui, B. Optogenetic control of intracellular signaling pathways. *Trends Biotechnol.* **2015**, *33*, 92−100.
(7) Fan, L. Z.; Lin, M. Z. Optical control of biological processes by light-switchable proteins. *Wiley Interdiscip. Rev.: Dev. Biol.* **2015**, *4*, 545−554.
(8) Repina, N. A.; Rosenbloom, A.; Mukherjee, A.; Schaffer, D. V.; Kane, R. S. At Light Speed: Advances in Optogenetic Systems for Regulating Cell Signaling and Behavior. *Annu. Rev. Chem. Biomol. Eng.* **2017**, *8*, 13−39.
(9) Yazawa, M.; Sadaghiani, A. M.; Hsueh, B.; Dolmetsch, R. E. Induction of protein-protein interactions in live cells using light. *Nat. Biotechnol.* **2009**, *27*, 941−945.
(10) Kennedy, M. J.; Hughes, R. M.; Peteya, L. A.; Schwartz, J. W.; Ehlers, M. D.; Tucker, C. L. Rapid blue-light-mediated induction of protein interactions in living cells. *Nat. Methods* **2010**, *7*, 973−975.
(11) Crefcoeur, R. P.; Yin, R.; Ulm, R.; Halazonetis, T. D. Ultraviolet-B-mediated induction of protein-protein interactions in mammalian cells. *Nat. Commun.* **2013**, *4*, 1779.
(12) Nihongaki, Y.; Suzuki, H.; Kawano, F.; Sato, M. Genetically Engineered Photoinducible Homodimerization System with Improved Dimer-Forming Efficiency. *ACS Chem. Biol.* **2014**, *9*, 617−621.
(13) Wang, H.; Vilela, M.; Winkler, A.; Tarnawski, M.; Schlichting, I.; Yumerefendi, H.; Kuhlman, B.; Liu, R.; Danuser, G.; Hahn, K. M. LOVTRAP: an optogenetic system for photoinduced protein dissociation. *Nat. Methods* **2016**, *13*, 755−758.
(14) Strickland, D.; Lin, Y.; Wagner, E.; Hope, C. M.; Zayner, J.; Antoniou, C.; Sosnick, T. R.; Weiss, E. L.; Glotzer, M. TULIPs: tunable, light-controlled interacting protein tags for cell biology. *Nat. Methods* **2012**, *9*, 379−384.
(15) Guntas, G.; Hallett, R. A.; Zimmerman, S. P.; Williams, T.; Yumerefendi, H.; Bear, J. E.; Kuhlman, B. Engineering an improved light-induced dimer (iLID) for controlling the localization and activity of signaling proteins. *Proc. Natl. Acad. Sci. U. S. A.* **2015**, *112*, 112−117.
(16) Motta-Mena, L. B.; Reade, A.; Mallory, M. J.; Glantz, S.; Weiner, O. D.; Lynch, K. W.; Gardner, K. H. An optogenetic gene expression system with rapid activation and deactivation kinetics. *Nat. Chem. Biol.* **2014**, *10*, 196−202.
(17) Zhou, X. X.; Chung, H. K.; Lam, A. J.; Lin, M. Z. Optical Control of Protein Activity by Fluorescent Protein Domains. *Science* **2012**, *338*, 810−814.
(18) Vogel, V.; Sheetz, M. Local force and geometry sensing regulate cell functions. *Nat. Rev. Mol. Cell Biol.* **2006**, *7*, 265.
(19) Beedle, A. E.; Williams, A.; Relat-Goberna, J.; Garcia-Manyes, S. Mechanobiology−chemical origin of membrane mechanical resistance and force-dependent signaling. *Curr. Opin. Chem. Biol.* **2015**, *29*, 87−93.
(20) Vandenburgh, H. H. Mechanical forces and their second messengers in stimulating cell growth in vitro. *Am. J. Physiol.: Regul., Integr. Comp. Physiol.* **1992**, *262*, R350−R355.
(21) Chicurel, M. E.; Chen, C. S.; Ingber, D. E. Cellular control lies in the balance of forces. *Curr. Opin. Cell Biol.* **1998**, *10*, 232−239.
(22) Sheetz, M. P.; Felsenfeld, D. P.; Galbraith, C. G. Cell migration: regulation of force on extracellular-matrix-integrin complexes. *Trends Cell Biol.* **1998**, *8*, 51−54.
(23) Discher, D. E.; Janmey, P.; Wang, Y.-l. Tissue Cells Feel and Respond to the Stiffness of Their Substrate. *Science* **2005**, *310*, 1139−1143.
(24) Lee, J.; Ishihara, A.; Oxford, G.; Johnson, B.; Jacobson, K. Regulation of cell movement is mediated by stretch-activated calcium channels. *Nature* **1999**, *400*, 382−386.
(25) Discher, D. E.; Mooney, D. J.; Zandstra, P. W. Growth Factors, Matrices, and Forces Combine and Control Stem Cells. *Science* **2009**, *324*, 1673−1677.
(26) Fu, J.; Wang, Y.-K.; Yang, M. T.; Desai, R. A.; Yu, X.; Liu, Z.; Chen, C. S. Mechanical regulation of cell function with geometrically modulated elastomeric substrates. *Nat. Methods* **2010**, *7*, 733−736.
(27) Elosegui-Artola, A.; Andreu, I.; Beedle, A. E.; Lezamiz, A.; Uroz, M.; Kosmalska, A. J.; Oria, R.; Kechagia, J. Z.; Rico-Lastres, P.; Roux, A.-L. L.; Shanahan, C. M.; Trepat, X.; Navajas, D.; Garcia-Manyes, S.; Roca-Cusachs, P. Force Triggers YAP Nuclear Entry by Regulating Transport across Nuclear Pores. *Cell* **2017**, *171*, 1397−1410.
(28) Dietz, H.; Rief, M. Exploring the energy landscape of GFP by single-molecule mechanical experiments. *Proc. Natl. Acad. Sci. U. S. A.* **2004**, *101*, 16192−16197.
(29) Ganim, Z.; Rief, M. Mechanically switching single-molecule fluorescence of GFP by unfolding and refolding. *Proc. Natl. Acad. Sci. U. S. A.* **2017**, *114*, 11052−11056.
(30) Saeger, J.; Hytönen, V. P.; Klotzsch, E.; Vogel, V. GFP's Mechanical Intermediate States. *PLoS One* **2012**, *7*, e46962.
(31) del Rio, A.; Perez-Jimenez, R.; Liu, R.; Roca-Cusachs, P.; Fernandez, J. M.; Sheetz, M. P. Stretching Single Talin Rod Molecules Activates Vinculin Binding. *Science* **2009**, *323*, 638−641.
(32) Zhou, X. X.; Fan, L. Z.; Li, P.; Shen, K.; Lin, M. Z. Optical control of cell signaling by single-chain photoswitchable kinases. *Science* **2017**, *355*, 836−842.
(33) Zhou, X. X.; Zou, X.; Chung, H. K.; Gao, Y.; Liu, Y.; Qi, L. S.; Lin, M. Z. A Single-Chain Photoswitchable CRISPR-Cas9 Architecture for Light-Inducible Gene Editing and Transcription. *ACS Chem. Biol.* **2018**, *13*, 443−448.
(34) Ando, R.; Mizuno, H.; Miyawaki, A. Regulated Fast Nucleocytoplasmic Shuttling Observed by Reversible Protein Highlighting. *Science* **2004**, *306*, 1370−1373.
(35) Habuchi, S.; Ando, R.; Dedecker, P.; Verheijen, W.; Mizuno, H.; Miyawaki, A.; Hofkens, J. Reversible single-molecule photoswitching in the GFP-like fluorescent protein Dronpa. *Proc. Natl. Acad. Sci. U. S. A.* **2005**, *102*, 9511−9516.
(36) Milles, L.; Gaub, H. Is mechanical receptor ligand dissociation driven by unfolding or unbinding? 2019, *biorxiv.org*, https://doi.org/10.1101/593335.
(37) Strackharn, M.; Pippig, D. A.; Meyer, P.; Stahl, S. W.; Gaub, H. E. Nanoscale Arrangement of Proteins by Single-Molecule Cut-and-Paste. *J. Am. Chem. Soc.* **2012**, *134*, 15193−15196.
(38) Ott, W.; Jobst, M. A.; Schoeler, C.; Gaub, H. E.; Nash, M. A. Single-molecule force spectroscopy on polyproteins and receptor-ligand complexes: The current toolbox. *J. Struct. Biol.* **2017**, *197*, 3−12.
(39) Jobst, M. A.; Schoeler, C.; Malinowska, K.; Nash, M. A. Investigating Receptor-ligand Systems of the Cellulosome with AFM-based Single-molecule Force Spectroscopy. *J. Visualized Exp.* **2013**, *82*, e50950.
(40) Schoeler, C.; Malinowska, K. H.; Bernardi, R. C.; Milles, L. F.; Jobst, M. A.; Durner, E.; Ott, W.; Fried, D. B.; Bayer, E. A.; Schulten, K.; Gaub, H. E.; Nash, M. A. Ultrastable cellulosome-adhesion complex tightens under load. *Nat. Commun.* **2014**, *5*, 5635.
(41) Ainavarapu, S. R. K.; Brujić, J.; Huang, H. H.; Wiita, A. P.; Lu, H.; Li, L.; Walther, K. A.; Carrion-Vazquez, M.; Li, H.; Fernandez, J. M. Contour Length and Refolding Rate of a Small Protein Controlled by Engineered Disulfide Bonds. *Biophys. J.* **2007**, *92*, 225−233.
(42) Dedecker, P.; Hotta, J.; Ando, R.; Miyawaki, A.; Engelborghs, Y.; Hofkens, J. Fast and Reversible Photoswitching of the Fluorescent Protein Dronpa as Evidenced by Fluorescence Correlation Spectroscopy. *Biophys. J.* **2006**, *91*, L45−L47.
(43) Bell, G. Models for the specific adhesion of cells to cells. *Science* **1978**, *200*, 618−627.
(44) Evans, E.; Ritchie, K. Dynamic strength of molecular adhesion bonds. *Biophys. J.* **1997**, *72*, 1541−1555.
(45) Schäfer, C.; Eckel, R.; Ros, R.; Mattay, J.; Anselmetti, D. Photochemical Single-Molecule Affinity Switch. *J. Am. Chem. Soc.* **2007**, *129*, 1488−1489.
(46) Anselmetti, D.; Bartels, F. W.; Becker, A.; Decker, B.; Eckel, R.; McIntosh, M.; Mattay, J.; Plattner, P.; Ros, R.; Schäfer, C.; Sewald, N. Reverse Engineering of an Affinity-Switchable Molecular Interaction Characterized by Atomic Force Microscopy Single-Molecule Force Spectroscopy. *Langmuir* **2008**, *24*, 1365−1370.

DOI: 10.1021/acs.nanolett.9b00639
Nano Lett. XXXX, XXX, XXX−XXX

(47) Walhorn, V.; Schäfer, C.; Schröder, T.; Mattay, J.; Anselmetti, D. Functional characterization of a supramolecular affinity switch at the single molecule level. *Nanoscale* **2011**, *3*, 4859−4865.
(48) Perez-Jimenez, R.; Garcia-Manyes, S.; Ainavarapu, S. R. K.; Fernandez, J. M. Mechanical Unfolding Pathways of the Enhanced Yellow Fluorescent Protein Revealed by Single Molecule Force Spectroscopy. *J. Biol. Chem.* **2006**, *281*, 40010−40014.
(49) Mizuno, H.; Mal, T. K.; Wälchli, M.; Kikuchi, A.; Fukano, T.; Ando, R.; Jeyakanthan, J.; Taka, J.; Shiro, Y.; Ikura, M.; Miyawaki, A. Light-dependent regulation of structural flexibility in a photochromic fluorescent protein. *Proc. Natl. Acad. Sci. U. S. A.* **2008**, *105*, 9227−9232.
(50) Austen, K.; Ringer, P.; Mehlich, A.; Chrostek-Grashoff, A.; Kluger, C.; Klingner, C.; Sabass, B.; Zent, R.; Rief, M.; Grashoff, C. Extracellular rigidity sensing by talin isoform-specific mechanical linkages. *Nat. Cell Biol.* **2015**, *17*, 1597.
(51) Moore, S. W.; Roca-Cusachs, P.; Sheetz, M. P. Stretchy Proteins on Stretchy Substrates: The Important Elements of Integrin-Mediated Rigidity Sensing. *Dev. Cell* **2010**, *19*, 194−206.
(52) Sun, Z.; Martinez-Lemus, L. A.; Trache, A.; Trzeciakowski, J. P.; Davis, G. E.; Pohl, U.; Meininger, G. A. Mechanical properties of the interaction between fibronectin and $\alpha 5\beta 1$-integrin on vascular smooth muscle cells studied using atomic force microscopy. *Am. J. Physiol.: Heart Circ. Physiol.* **2005**, *289*, H2526−H2535.
(53) Ferrer, J. M.; Lee, H.; Chen, J.; Pelz, B.; Nakamura, F.; Kamm, R. D.; Lang, M. J. Measuring molecular rupture forces between single actin filaments and actin-binding proteins. *Proc. Natl. Acad. Sci. U. S. A.* **2008**, *105*, 9221−9226.
(54) Grashoff, C.; Hoffman, B. D.; Brenner, M. D.; Zhou, R.; Parsons, M.; Yang, M. T.; McLean, M. A.; Sligar, S. G.; Chen, C. S.; Ha, T.; Schwartz, M. A. Measuring mechanical tension across vinculin reveals regulation of focal adhesion dynamics. *Nature* **2010**, *466*, 263−266.
(55) Echelman, D. J.; Alegre-Cebollada, J.; Badilla, C. L.; Chang, C.; Ton-That, H.; Fernández, J. M. CnaA domains in bacterial pili are efficient dissipaters of large mechanical shocks. *Proc. Natl. Acad. Sci. U. S. A.* **2016**, *113*, 2490−2495.
(56) Milles, L. F.; Schulten, K.; Gaub, H. E.; Bernardi, R. C. Molecular mechanism of extreme mechanostability in a pathogen adhesin. *Science* **2018**, *359*, 1527−1533.
(57) Zimmermann, J. L.; Nicolaus, T.; Neuert, G.; Blank, K. Thiol-based, site-specific and covalent immobilization of biomolecules for single-molecule experiments. *Nat. Protoc.* **2010**, *5*, 975−985.
(58) Yin, J.; Straight, P. D.; McLoughlin, S. M.; Zhou, Z.; Lin, A. J.; Golan, D. E.; Kelleher, N. L.; Kolter, R.; Walsh, C. T. Genetically encoded short peptide tag for versatile protein labeling by Sfp phosphopantetheinyl transferase. *Proc. Natl. Acad. Sci. U. S. A.* **2005**, *102*, 15815−15820.
(59) Gumpp, H.; Stahl, S. W.; Strackharn, M.; Puchner, E. M.; Gaub, H. E. Ultrastable combined atomic force and total internal fluorescence microscope. *Rev. Sci. Instrum.* **2009**, *80*, 063704.
(60) Bustamante, C.; Marko, J.; Siggia, E.; Smith, S. Entropic elasticity of lambda-phage DNA. *Science* **1994**, *265*, 1599−1600.

DOI: 10.1021/acs.nanolett.9b00639
Nano Lett. XXXX, XXX, XXX−XXX